Zhang et al. Nanoscale Research Letters (2016) 11:5
DOI 10.1186/s11671-015-1207-6

Nanoscale Research Letters
a SpringerOpen Journal

NANO EXPRESS Open Access

Wide-range Vacuum Measurements from MWNT Field Emitters Grown Directly on Stainless Steel Substrates

Jian Zhang[1], Detian Li[1,2*], Yangyang Zhao[1], Yongjun Cheng[2] and Changkun Dong[1,2*]

Abstract

The field emission properties and the vacuum measurement application are investigated from the multi-walled carbon nanotubes (MWNTs) grown directly on catalytic stainless steel substrates. The MWNT emitters present excellent emission properties after the acid treatment of the substrate. The MWNT gauge is able to work down to the extreme-high vacuum (XHV) range with linear measurement performance in wide range from 10^{-11} to 10^{-6} Torr. A modulating grid is attempted with improved gauge sensitivity. The extension of the lower pressure limit is attributed largely to low outgassing effect due to direct growth of MWNTs and justified design of the electron source.

Keywords: Field emission, Carbon nanotube, Ionization gauge, Ultra-high vacuum, Modulator

Background

The electron field emission has potential to overcome thermionic emission related problems [1–4] for merits such as room-temperature operation, low power consumption, and quick response capability. Carbon nanotubes (CNTs) possess unique electrical, chemical, and mechanical as well as structural properties and are regarded as the most promising field emission material with low emission fields and good vacuum behaviors [5–14]. The "cold" cathode operation could help to reduce the outgassings, benefiting greatly the ultra-high vacuum/extreme-high vacuum (UHV/XHV) measurement. Many investigations have been conducted to employ the CNT field emission in ionization gauge applications. Murakami et al. presented a Bayard-Alpert type CNT field emission gauge and tested in 10^{-6} to 10^{-4} Torr range [15]. In 2004, Dong and Myneni developed an extractor type field emission gauge based on the MWNTs grown on Ni alloy. The gauge presented excellent measurement linearity from 10^{-10} to 10^{-6} Torr with the sensitivity of about 3 $Torr^{-1}$ [16, 17]. Huang et al. replaced thermionic filament of the Bayard-Alpert gauge (BAG) by a line-type CNT cathode, and the gauge performances were studied from 10^{-4} to 10^{-7} Torr with the sensitivity of 3.6 $Torr^{-1}$ [18]. Suto et al. developed the CNT electron source by screen printing and studied its ionization gauge application [19].The gauge responded linearly from 10^{-8} to 10^{-4} Torr with the sensitivity of 13 $Torr^{-1}$, close to the commercial gauge sensitivity. New gauge designs and structural modulations were also attempted. Sheng et al. constructed a saddle field gauge with a simple ring anode. The gauge was tested from 10^{-5} to 10^{-3} Pa with improved sensitivity of 1.7 Pa^{-1} [20]. A simple triode type of CNT ionization gauge was investigated by several groups, but there were no UHV/XHV measurement results [21–25].

The applications of CNT field emission in pressure measurement have not been well established. Some technical issues, including the outgassings due to the breaking off of the film components and the gas desorption from the CNT cathode, restrict the UHV/XHV applications. In this work, MWNTs are grown directly on the stainless steel substrate (S.S.) without extra catalyst layer by thermal chemical vapor deposition (CVD). Improved field emission performances are presented from the MWNT emitters after anodizing the substrate. The all mechanical assembly MWNT field emission cathode is constructed with low emission fields, high electron transmittances over the gate, and long-term stability. The ionization gauge behaviors based on the MWNT source

* Correspondence: lidetian@hotmail.com; dck@wzu.edu.cn
[1]Institute of Micro-nano Structures and Optoelectronics, Wenzhou University, Chashan University Town, Wenzhou, China
Full list of author information is available at the end of the article

are investigated with excellent measurement linearity from 10^{-11} to 10^{-6} Torr.

Methods

The MWNT film is grown directly on the 304 S.S. without extra catalyst layer by the CVD technique from C_2H_2/Ar source gases at 750 °C. To improve the field emission properties, the S.S. substrate is anodized in the 0.3 mol L^{-1} oxalic acid solution. The field emission properties are compared for regular and anodized MWNT emitters from the diode setup. By screwing the parts together without any adhesive material, MWNT electron source is developed from totally mechanical assembly with features of low outgassing rates, good emission stability, and the feasibility to replace the MWNT cathode. The MWNT field emission ionization gauge is constructed upon the extractor gauge. The gauge performances are investigated inside a turbo vacuum system with 10^{-11} Torr background vacuum, and the pressure is calibrated against a commercial IE 514 extractor gauge. The measurement linearities are investigated for N_2, H_2, and O_2, respectively, in wide pressure ranges. Keithley multimeters are used to supply the operation potentials and measure ion and electron currents.

Results and Discussion

Figure 1a and b shows SEM images of the randomly oriented MWNTs grown on regular and anodized S.S. substrates, respectively. It is clear that the anodization process improves the CNT diameter uniformity, the density, and the straightness significantly. The average tube diameter is also smaller. According to the histogram plot of Fig. 1c counting on the nanotube diameters for Fig. 1b, the MWNTs of diameters in 30–50 nm account for 80 %. The analysis of the surface morphology shows that more uniform and higher density nano-scale pores appear after anodization comparing with the regular substrate, favoring the CNT growth, as shown in AI-1 of Additional file 1.

Field emission J-E and stability behaviors of MWNT films are tested, as shown in Fig. 2. After the anodization,

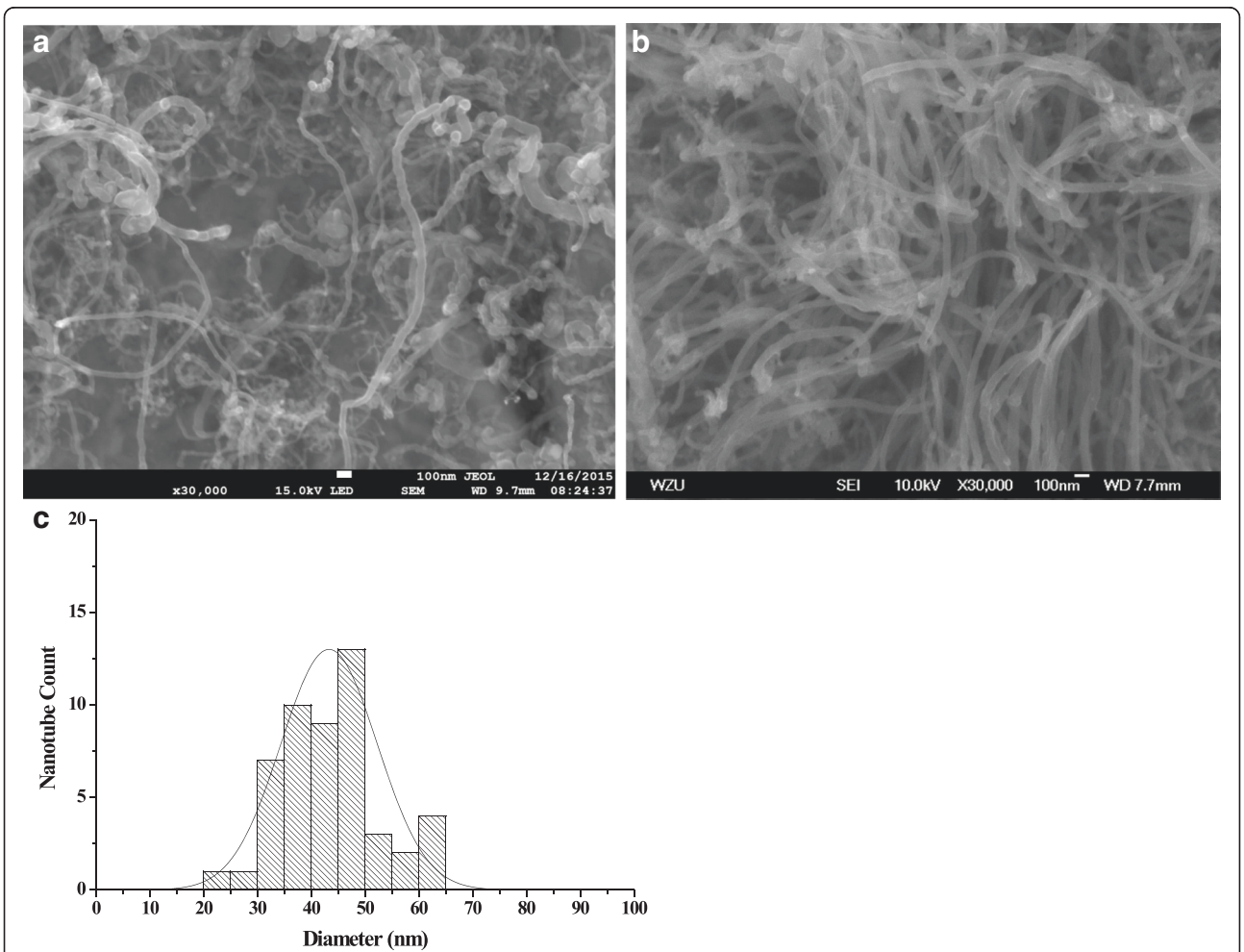

Fig. 1 SEM images of MWNT emitters grown on the stainless steel substrate. **a** Regular sample. **b** After substrate anodization. **c** Histograms of the nanotubes diameter distribution corresponding to (**b**)

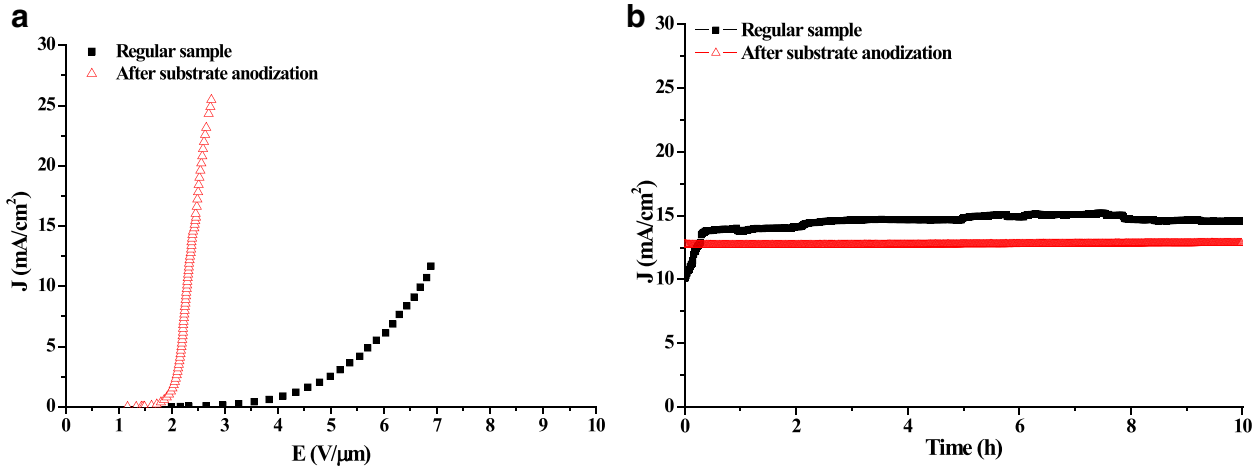

Fig. 2 Emission improvements after the substrate anodization. **a** Emission current density-field curves. **b** Emission stabilities tested in 10^{-8} Torr

the turn-on field drops from 2.2 to 1.4 V μm^{-1}, and the threshold field drops from 6.68 to 2.28 V μm^{-1}. Meanwhile, the emission under the current density of 12 mA cm^{-2} is more stable with the fluctuation of less than ±0.5 % in 10^{-8} Torr. The significant reductions of the emission fields are probably related to the decrease of the MWNT diameter and the increase of emission sites, where better straightness of the MWNT emitters are regarded as the key factor for the excellent emission stability after the anodization.

The structure of the MWNT electron source is illustrated in Fig. 3a. The extraction gate of 92.2 % transmittance tungsten gauze is separated from the MWNT cathode by a 100 μm aluminum oxide ceramic plate. An optional mesh modulator, which adjusts the electron energy to improve the measurement sensitivity, is also attempted in this study. The MWNT field emission ionization gauge is demonstrated in Fig. 3b, where the MWNT source is mounted 2 mm above the anode grid. The top source layout benefits the elongation of the electron trajectory to improve the gauge sensitivity [17, 26, 27]. The MWNT source exhibits excellent emission properties while integrating into the gauge. As shown in Fig. 4a, the emission current of 74 μA is reached under the gate potential of 350 V with the electron transmittance (anode current I_e/cathode current I_c) of about 60 %. Beyond the physical structure and the extraction field, the anode potential brings about significant impacts on the electron transmittance. The transmittance (I_e/I_c) increases from 38.2 to 74.4 % when the anode/gate potential ratio V_a/V_g varies from 1:1 to 2:1, as shown in Fig. 4b. The anode potential could penetrate through the gate grid to enhance the extraction field and also assists the electron flying off the gate grid. The electron source exhibits good emission stability behaviors in wide pressure range. However, the current fluctuation increases to ±4.24 % in 2.59×10^{-9} Torr vacuum, comparing with ±2.72 % in 2.48×10^{-10} Torr, which is believed to be related to the gas adsorption, such as nitrogen and hydrogen [16, 28].

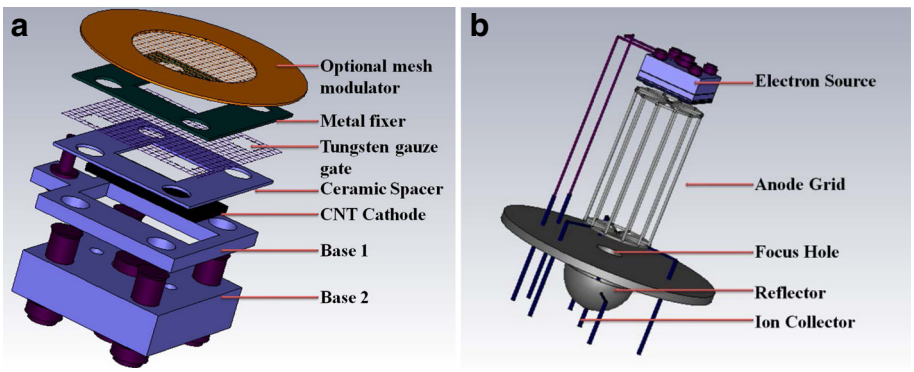

Fig. 3 **a** Schematic drawing of the electron source with an optional mesh modulator. **b** Illustration of the MWNT ionization gauge with the spacing between the electron source and the anode of 2 mm

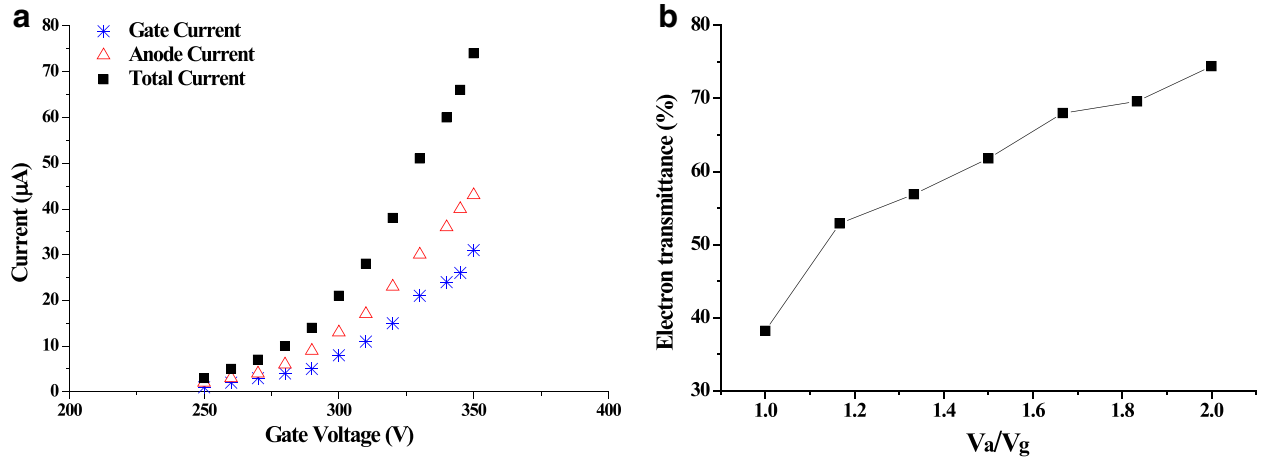

Fig. 4 Emission characteristics of the electron source with the MWNT emission area of 20 mm^2 and the cathode-gate spacing of 100 μm. **a** I-V curves under cathode-anode spacing of 2 mm and anode voltage of 430 V. **b** Electron transmittances over the gate grid with the increase of V_a/V_g ratios

The working principle of the ionization gauge is described by the relationship [29]: $I_i/I_e = K^*P$, where I_i is the ion current, I_e is the electron current (for the MWNT gauge, I_e is the anode current), P is the pressure, K is the gauge sensitivity factor, and the ratio I_i/I_e is defined as the normalized ion current. K depends on the structural and the electric properties of the gauge. Figure 5a shows the calibration curves between the normalized ion current and pressure in different gas environments. The MWNT gauge presents excellent measurement linearity from 10^{-11} to 10^{-6} Torr with the sensitivity factor of about 2.22 $Torr^{-1}$ for nitrogen. To our knowledge, this is the lowest lower pressure measurement limit reached in the reports for the CNT field emission ionization gauges. This excellent UHV measurement performance is benefited from the advantageous MWNT grown technique and the electron source design, which enable the low outgassings from the electron source. Further extension of the lower pressure measurement limit is subject to the accurate measurements of very weak ion current signals. The MWNT gauge also shows good measurement linearities for hydrogen and oxygen gases. Due to lower ionization efficiency, the sensitivity factor with hydrogen is about one third of the value with nitrogen. The oxygen calibration curve is slightly lower than nitrogen curve owing to the similarity of the ionization efficiencies between two gas species [30–32].

The gauge outgassing property, including the electron stimulated desorption (ESD) effect, plays a key role for the measurement accuracy and the XHV feasibility. This MWNT ionization gauge exhibits excellent low outgassing behaviors, leading to the superior measurement

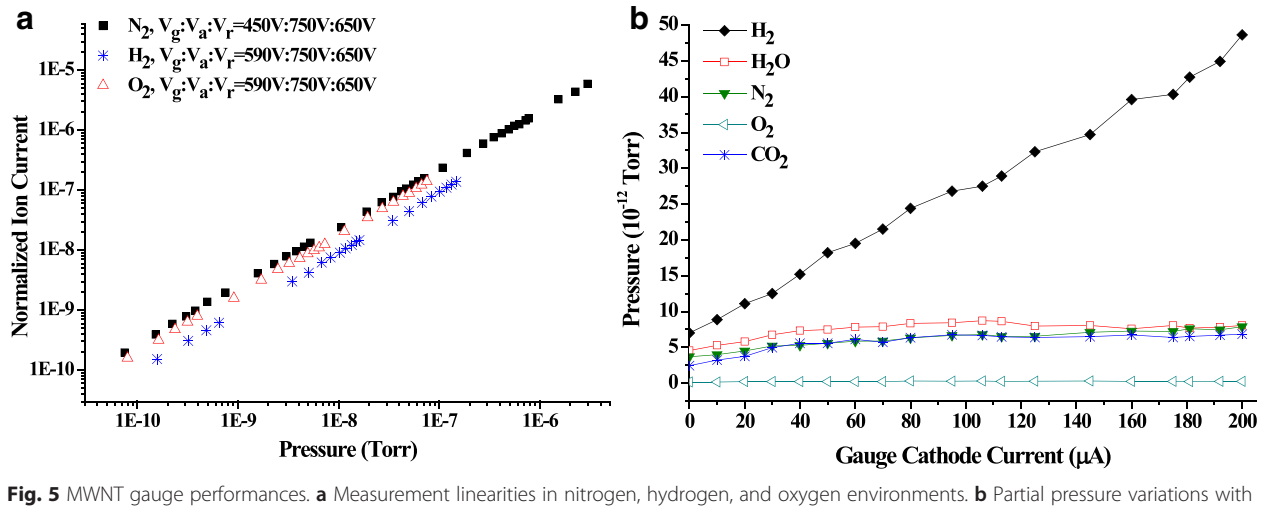

Fig. 5 MWNT gauge performances. **a** Measurement linearities in nitrogen, hydrogen, and oxygen environments. **b** Partial pressure variations with the increase of emission current

performance. Under the emission current of 100 μA, the system pressure may go up about 2×10^{-10} Torr in the 10^{-11} Torr vacuum. After the electrode cleaning from the higher emission flashing, i.e., 200 μA for a couple of minutes, the pressure rise could be smaller than 7×10^{-11} Torr. The electron bombardment cleans the surface adsorptions effectively. The outgassing properties for different gas species are further investigated. Figure 5b shows the partial pressure variations with increasing the emission current up to 200 μA. Hydrogen accounts for the major gas kind, which increases roughly linearly from 7.01×10^{-12} to 4.86×10^{-11} Torr. The steady rise of the hydrogen partial pressure is believed to be related to H_2 desorptions from interiors of the metal electrodes due to the temperature rise by electron bombardments [33, 34]. With increasing the emission to 106 μA, partial pressures of H_2O, N_2, CO_2, and O_2 increase from 4.57×10^{-12} to 8.72×10^{-12} Torr (91 %), 3.69×10^{-12} to 6.78×10^{-12} Torr (84 %), 2.46×10^{-12} to 6.68×10^{-12} Torr, and 1.47×10^{-13} to 3.0×10^{-13} Torr, respectively, and reach stable states or drop afterwards. The gentle ascents for these four gases before 100 μA are ascribed to surface outgassings. The low outgassing performance, which enables the extension of the lower pressure limit to 10^{-11} Torr level, is attributed to several aspects, including the mechanical assembly of the cathode consisting of low outgassing materials, low extraction potentials, and the direct growth of MWNT emitters without extra gas adsorption materials.

The measurement sensitivity is determined by several factors, including the gas species, the gauge structure, and the electrode potentials. After balancing several key characteristic properties, including high ionization efficiency and low outgassing rates, the thermionic cathode ionization gauges are commonly designed to maintain the electron energies at around 150~200 V [3, 32, 35]. For the field emission based gauge, the electron energies are normally higher due to the existence of high electron extraction field [16, 18, 36]. The variations of the

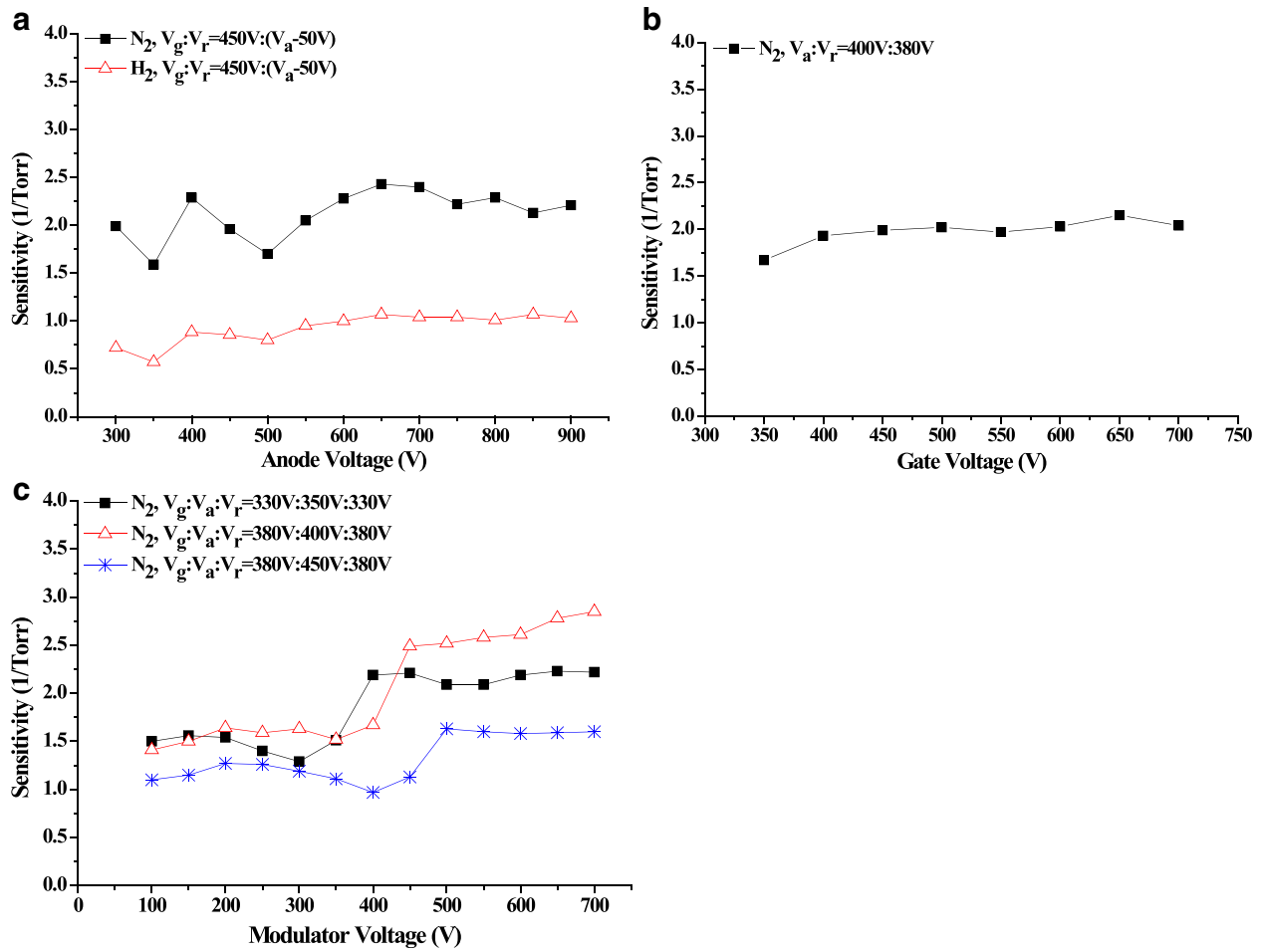

Fig. 6 Sensitivity behaviors of the MWNT gauge. **a** Sensitivity and anode potential relations for nitrogen and hydrogen. **b** Sensitivity and gate potential relation for nitrogen. **c** Sensitivity and the modulator potential relations

sensitivity factor K with the increases of the anode and the gate potentials are illustrated in Fig. 6. When varying the anode potential, the K for nitrogen bumps up and down and reaches the maximum value of 2.43 $Torr^{-1}$ at 650 V, and K with hydrogen changes in the same rhythm. The fluctuations of the sensitivities could be related to the electron trajectories which are influenced by the electric field distribution [26]. While keeping the anode potential constant and raising the gate potential, K also rises and reaches 2.15 $Torr^{-1}$ at 650 V. The increase of sensitivity factor with the potential is believed to be related to the elongations of the electron trajectories [20, 26, 35], even though the ionization efficiencies of major air components, i.e., N_2, H_2, and O_2, drop beyond energies of 200 eV.

The improvement of the sensitivity factor is particularly important to extend the measurement down to UHV/XHV range where ion collection currents are normally extremely small. To evaluate the sensitivity performance by modulating the electron energy, the role of a mesh modulator with 92.2 % physical transparency is investigated. As shown in Fig. 6c, the relations between K and the modulator potential are tested for three anode potentials of 350, 400, and 450 V, respectively. With increasing the modulator potential from 100 to 700 V, the sensitivity factor varies roughly in two plateaus, and a transition leap occurs when the modulator potential is equal to and 50 V higher than the anode potential. Further increase of the modulator potential does not improve the K factor significantly. This leap is most probably related to the prolongations of the electron trajectories because a slightly higher modulator potential assists the electrons move back and forth around the top of the anode grid. Under the anode potential of 400 V, K reaches 2.85 $Torr^{-1}$, 20 % higher than the value without the modulator. Liu et al. also demonstrated the sensitivity improvement by a shield electrode for the CNT BA gauge [37]. Therefore, the electron energy modulation enhances the gauge measurement sensitivity effectively.

Conclusions

In summary, we have developed a carbon nanotube field emission ionization gauge after growing MWNTs directly on stainless steel substrates. The MWNT cathode presents excellent emission J-E and stability performances after the substrate anodization. The MWNT gauge demonstrates excellent measurement linearity in wide pressure range with the lower measurement limit down to 10^{-11} Torr, attributed largely to low outgassings due to the direct growth of MWNTs. The modulation of the electron energy benefits the improvement of the measurement performance. This gauge shows potential for UHV/XHV pressure measurements.

Additional file

Additional file 1: Additional information. Substrate surface morphology variations after anodization and the residual gas mass spectroscopy of the experimental system. (DOCX 322 kb)

Competing interests

The authors declare that they have no competing interests.

Authors' contributions

DL, CD, and YC conceived the idea. CD and JZ designed the experiments. JZ performed the experiments. CD, JZ, DL, and YZ analyzed the data. JZ and CD co-wrote the manuscript and all authors discussed the results. All authors read and approved the final manuscript.

Acknowledgements

This work is supported by the NSF of China (Grants No. 11274244, No. 61125101) and the Scientific Research Foundation for the Returned Overseas Chinese Scholars.

Author details

[1]Institute of Micro-nano Structures and Optoelectronics, Wenzhou University, Chashan University Town, Wenzhou, China. [2]Science and Technology on Vacuum Technology and Physics Laboratory, Lanzhou Institution of Physics, Lanzhou, China.

Received: 13 October 2015 Accepted: 21 December 2015
Published online: 06 January 2016

References

1. Redhead PA (1981) Foundations of vacuum science and technology. Wiley, New York, pp 625–642
2. Irako M, Oguri T, Kanomata I (1975) Static operation mass-spectrometer. Japanese Journal of Applied Physics 14(4):533–543
3. Peacock RN, Peacock NT, Hauschulz DS (1991) Comparison of hot cathode and cold cathode ionization gauges. Journal of Vacuum Science & Technology A 9:1977–1985
4. Baptist R, Bieth C, Py C (1996) Bayard-Alpert vacuum gauge with microtips. Journal of Vacuum Science & Technology B 14(3):2119–2125
5. Yung Jr H, Yung Jui H, Hsuan Chen C, Kuei Yi L, San Liang L (2014) Patterned growth of carbon nanotube over vertically aligned silicon nanowire bundles for achieving uniform field emission. Nanoscale Research Letters 9:451
6. Abdalla S, Al Marzouki F, Ahmed A, Al G, Abdel Daiem A (2015) Different technical applications of carbon nanotubes. Nanoscale Research Letters 10:358
7. Pao Hung L, Cong Lin S, Ching An C, Hsuan Chen C, Yi Ting S, Hsin Yueh C, Wei Jhih S, Kuei Yi L (2015) Field emission characteristics of the structure of vertically aligned carbon nanotube bundles. Nanoscale Research Letters 10:297
8. Sridhar S, Ge L, Tiwary CS, Hart AC, Ozden S, Kalaga K, Lei S, Sridhar SV, Sinha RK, Harsh H, Kordas K, Ajayan PM, Vajtai R (2014) Enhanced field emission properties from CNT arrays synthesized on inconel superalloy. ACS Applied Materials and Interfaces 6(3):1986–1991
9. Dong Hoon S, Seung Il J, Ki Nam Y, Guohai C, Yoon-Ho S, Yahachi S, Milne WI, Cheol Jin L (2014) Field emission properties from flexible field emitters using carbon nanotube film. Applied Physics Letters 105(3):033110
10. Sridhar S, Tiwary C, Vinod S, Taha-Tijerina JJ, Sridhar S, Kalaga K, Sirota B, Hart AH, Ozden S, Sinha RK, Harsh, Vajtai R, Choi W, Kordás K, Ajayan PM (2014) Field emission with ultralow turn on voltage from metal decorated carbon nanotubes. ACS Nano 8(8):7763–7770
11. Lee JS, Kim T, Kim SG, Cho MR, Seo DK, Lee M, Kim S, Kim DW, Park GS, Jeong DH, Park YD, Yoo JB, Kang TJ, Kim YH (2014) High performance CNT point emitter with graphene interfacial layer. Nanotechnology 25(45):455601
12. Jian Hua D, Xing Gang H, Lin C, Fan Jie W, Bin Y, Guo Zheng L, De Jun L, Guo An C, Shaolong W (2014) Irradiation damage determined field emission of ion irradiated carbon nanotubes. ACS Applied Materials and Interfaces 6(7):5137–5143
13. Rémi L, Juan Ramon S-V, Shorubalko I, Furrer R, Hack E, Elsener H, Gröning O, Greenwood P, Rupesinghe N, Teo K, Leinenbach C, Gröning P (2015)

Active vacuum brazing of CNT films to metal substrates for superior electron field emission performance. Science and Technology of Advanced Materials 16(1):15005–15015
14. Kar R, Sarkar SG, Basak CB, Avinash P, Sandip D, Chanchal G, Divakar R, Chand N, Chopade SS, Patil DS (2015) Effect of substrate heating and microwave attenuation on the catalyst free growth and field emission of carbon nanotubes. Carbon 94:256–265
15. Murakami H, Iwata T, Machida K (2001) Preliminary test of a carbon nanotubes vacuum gauge for space use. Shinku 44:671–674
16. Dong C, Gupta M (2003) Influences of the surface reactions on the field emission from multiwall carbon nanotubes. Applied Physics Letters 83(1):159–161
17. Dong C, Myneni GR (2004) Carbon nanotube electron source based ionization vacuum gauge. Applied Physics Letters 84(26):5443–5445
18. Huang JX, Jun C, Deng SZ, NS X (2007) Bayard-Alpert ionization gauge using carbon-nanotube cold cathode. Journal of Vacuum Science and Technology B 25(2):651–654
19. Suto H, Fujll S, Yoshihara K, Ishidai K, Tanaka Y, Honda SI, Katayama M (2008) Fabrication of cold cathode ionization gauge using screen-printed carbon nanotube field electron emitter. Japanese Journal of Applied Physics 47(4):2032–2035
20. Sheng L, Liu P, Yang W, Liang L, Qi J, Fan S (2005) A saddle-field gauge with carbon nanotube field emitters. Diamond and Related Materials 14(10):1695–1699
21. Choi IM, Woo SY (2005) Application of carbon nanotube field emission effect to an ionization gauge. Applied Physics Letters 87(17):173104
22. Yang YC, Qian L, Tang J, Liu L, Fan SS (2008) A low-vacuum ionization gauge with HfC-modified carbon nanotubes field emitters. Applied Physics Letters 92(15):153105
23. Bower CA, Gilchrist KH, Piascik JR, Stoner BR, Natarajan S, Parker CB, Wolter SD, Glass JT (2007) On-chip electron-impact ion source using carbon nanotube field emitters. Applied Physics Letters 90(12):124102–124104
24. Su J, Guo DZ, Xing YJ, Zhang GM (2013) Improved field emission properties of MgO-nanoparticle-doped carbon nanotube films and their application in miniature vacuum gauges. Physica Status Solidi (a) 210(2):349–355
25. Dong KY, Lee YD, Kang BH, Choi J, Ju BK (2013) Design of a multi-walled carbon nanotube field emitter with micro vacuum gauge. Nanoscale Research Letters 8:143
26. Zhang H, Li D, Dong C, Yong Jun C, Yu Hua X (2013) Numerical simulation of electrode potential influence on the performance of ionization gauge with carbon nanotubes cathode. Acta Physica Sinica 62(11):110703
27. Changkun dong: field emission based sensors using carbon nanotubes. PhD thesis,Old Dominion University 2003.
28. Seong Chu L, Young Chul C, Hee Jin J, Young Min S, Kay Hyeok A, Dong Jae B, Young Hee L, Nae Sung L, Jong Min K (2001) Effect of gas exposure on field emission properties of carbon nanotube arrays. Advanced Materials 13(20):1563–1567
29. Redhead PA, Hobson JP, Kornelsen EV (1968) The physical basis of ultrahigh vacuum. Chapman and Hall Ltd., London, London
30. Compton KT, Van Voorhis CC (1925) Probability of ionization of gas molecules by electron impacts. Physical Review 26(4):436–453
31. Tate JT, Smith PT (1932) The efficiencies of ionization and ionization potentials of various gases under electron impact. Physical Review 39(2):270–277
32. Schulte M, Schlosser B, Seidel W (1994) Ionization gauge sensitivities of N_2, O_2, N_2O, NO, NO_2, NH_3, $CClF_3$ and CH_3OH. Fresenjus J Anal Chem 348(11):778–780
33. Lim SC et al (2006) A stategy for forming robust adhesion with the substrate in a carbon nanotube field emission array. Carbon 44:2809–2815
34. Bernardini M, Malter L (1965) Vacuum problems of electron and positron storage rings. Journal of vacuum science and technology 2(3):130–141
35. Pittaway LG (1970) Electron trajectories in ionization gauges. Journal of Physics D: Applied Physics 3(7):1113–1121
36. Lin X, Li Q, Yang W, Liang L, Shoushan F (2008) Conventional triode ionization gauge with carbon nanotube cold electron emitter. Journal of Vacuum Science and Technology A: Vacuum, Surfaces and Films 26(1):1–4
37. Liu H, Nakahara H, Uemura S, Saito Y (2010) Ionization vacuum gauge with a carbon nanotube field electron emitter combined with a shield electrode. Vacuum 84:713–717